ACS SyntheticBiology

pubs.acs.org/synthbio Research Article

Engineering Single Pan-Specific Ubiquibodies for Targeted Degradation of All Forms of Endogenous ERK Protein Kinase

Erin A. Stephens, Morgan B. Ludwicki, Bunyarit Meksiriporn, Mingji Li, Tianzheng Ye, Connor Monticello, Katherine J. Forsythe, Lutz Kummer, Pengbo Zhou, Andreas Plückthun, and Matthew P. DeLisa*

Cite This: *ACS Synth. Biol.* 2021, 10, 2396–2408 Read Online

ACCESS | Metrics & More | Article Recommendations | Supporting Information

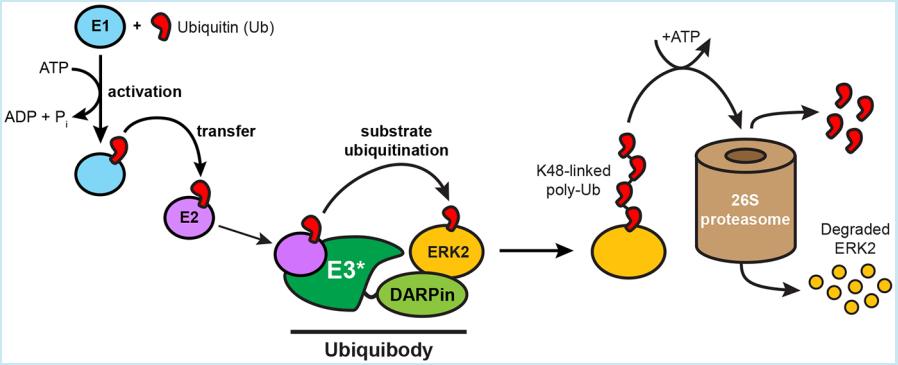

ABSTRACT: Ubiquibodies (uAbs) are a customizable proteome editing technology that utilizes E3 ubiquitin ligases genetically fused to synthetic binding proteins to steer otherwise stable proteins of interest (POIs) to the 26S proteasome for degradation. The ability of engineered uAbs to accelerate the turnover of exogenous or endogenous POIs in a post-translational manner offers a simple yet robust tool for dissecting diverse functional properties of cellular proteins as well as for expanding the druggable proteome to include tumorigenic protein families that have yet-to-be successfully drugged by conventional inhibitors. Here, we describe the engineering of uAbs composed of human carboxyl-terminus of Hsc70-interacting protein (CHIP), a highly modular human E3 ubiquitin ligase, tethered to differently designed ankyrin repeat proteins (DARPins) that bind to nonphosphorylated (inactive) and/or doubly phosphorylated (active) forms of extracellular signal-regulated kinase 1 and 2 (ERK1/2). Two of the resulting uAbs were found to be global ERK degraders, pan-specifically capturing all endogenous ERK1/2 protein forms and redirecting them to the proteasome for degradation in different cell lines, including MCF7 breast cancer cells. Taken together, these results demonstrate how the substrate specificity of an E3 ubiquitin ligase can be reprogrammed to generate designer uAbs against difficult-to-drug targets, enabling a modular platform for remodeling the mammalian proteome.

KEYWORDS: *DARPins, E3 ubiquitin ligase, protein degrader, targeted protein degradation, ubiquibodies, nonantibody scaffolds*

INTRODUCTION

Proteome editing technology has emerged as a powerful approach to control protein function at the post-translational level. Proteome editing involves a molecular degrader that hijacks the cellular quality control machinery to selectively eliminate target proteins, thereby executing an "inhibition-by-degradation" mechanism.[1−3] A common feature of proteome editing approaches is the ability to promote catalytic turnover of otherwise stable intracellular proteins, requiring only transient binding to virtually any site on the protein of interest (POI). This is in stark contrast to traditional occupancy-type inhibitors, which depend on a distinct binding site that affects function (*e.g.*, enzyme active site) and requires relatively high concentrations to ensure sustained stoichiometric binding. For these reasons, the development of proteome editors that are capable of inducing protein degradation is gaining considerable attention as a tool for studying native protein function as well as a therapeutic modality for targeting disease-relevant proteins, especially those that are recalcitrant to conventional pharmacological interventions and have thus been deemed difficult-to-drug.[4,5]

The creation of customized degrader molecules typically involves precision tagging of POIs so that they are redirected

Received: July 28, 2021
Published: August 16, 2021

https://doi.org/10.1021/acssynbio.1c00357
ACS Synth. Biol. 2021, 10, 2396–2408

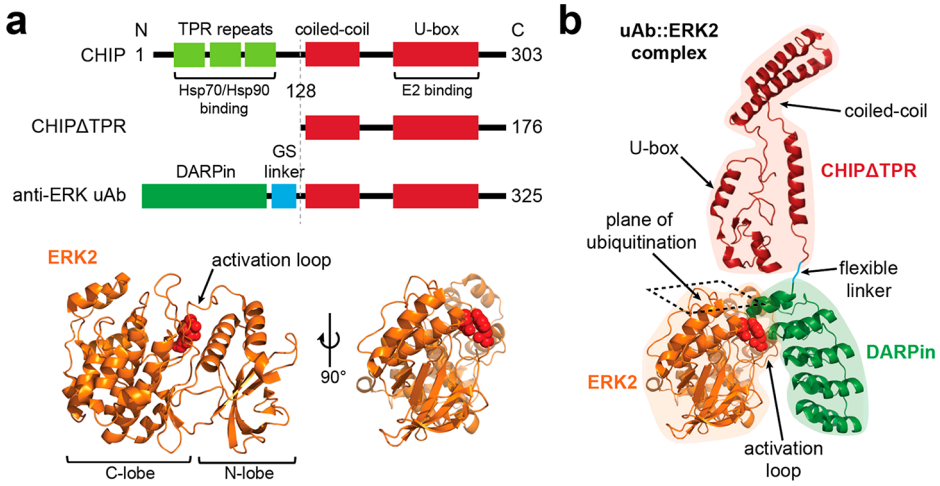

Figure 1. Modular design of a pan-specific ERK degrader. (a) The architecture of uAbs is highly modular, involving three distinct domains: a substrate-binding domain composed of a synthetic binding protein (green); a flexible Gly−Ser−Gly−Ser−Gly (GS) linker (blue); a catalytic domain composed of the C-terminus of human CHIP starting from residue 128 (CHIPΔTPR) (red). The synthetic binding domains used in this study are DARPins with specificity for different ERK forms. Crystal structure of human ERK2 (orange) generated in PyMOL (PDB ID: 3ZU7). Residues T185 and Y187 (red balls) are phosphorylated upon activation, leading to the rotation of the N-lobe with respect to the C-lobe. (b) Orientation of the catalytic domain in the uAb::ERK2 complex. The ubiquitination plane is in direct proximity to the theoretical position of the catalytic domain. Schematic generated from a composite of PDB IDs 2C2L and 3ZU7 in PyMOL and Illustrator software.

to natural degradation mechanisms common to all eukaryotic cell types. The most frequently exploited of these degradation processes is the ubiquitin-proteasome pathway (UPP), which involves the coordinated activity of three enzymes, ubiquitin-activating enzyme (E1), ubiquitin-conjugating enzyme (E2), and ubiquitin ligase (E3), that cooperate in an energy-dependent manner to covalently tag available lysines on protein targets with a polyubiquitin chain.[6] While a variety of polyubiquitin chain topologies are possible, K48-linked ubiquitin serves as the canonical recognition signal for the 26S proteasome and generally leads to substrate degradation.[7] The fact that E3s govern substrate specificity and often exhibit remarkable plasticity has made these enzymes the component of choice in the majority of proteome editing technologies described to date. Most notable among these technologies is PROTACs (proteolysis targeting chimeras),[8,9] which are heterobifunctional small molecules that effectively bridge the E3 and the POI, forming a ternary complex that facilitates polyubiquitination and subsequent proteasomal degradation of target proteins in cultured cells and mice.[10−14] With respect to clinical potential, two PROTACs, namely, ARV-110 that targets the androgen receptor and ARV-471 that targets the estrogen receptor, have entered into phase I human trials.[15]

Alongside small-molecule PROTACs are protein-based chimeras in which an E3 is genetically fused to a peptide or protein with affinity for the POI. In the earliest designs, substrate targeting was achieved by leveraging naturally occurring protein interaction partners, whereby fusion of an E3 (or a component of an E3 ligase complex) to a POI's known binding partner yielded a chimera that promoted knockout of the cognate POI following expression in cultured cells.[16,17] When a binding partner for a given POI is available, this approach has proven to be highly effective both *in vitro* and *in vivo*, leading to induced degradation of several different oncoprotein targets including c-Myc, ErbB, HIF-α, and KRAS.[18−21] However, this approach is limited to only those POIs for which a natural interacting partner is known.

Therefore, to extend this approach beyond naturally occurring protein−protein interactions, we created ubiquibodies (uAbs) by genetically fusing an E3 ubiquitin ligase to different synthetic binding proteins, including a DARPin (designed ankyrin repeat protein), an FN3 (fibronectin type III) monobody, and an scFv (single-chain antibody fragment), that specifically recognized the POIs of our choice.[22] Because synthetic binders can be readily identified using methods such as phage, ribosome, and yeast display[23,24] with the potential for proteome-scale coverage,[25] uAbs are a universally applicable technology that can be developed against virtually any intracellular POI. Indeed, by combining the flexible ubiquitin-tagging capability of human CHIP (carboxyl-terminus of Hsc70-interacting protein), a RING/U-box-type E3 ubiquitin ligase, with the programmable affinity and specificity of synthetic binding proteins, we demonstrated that uAbs efficiently redirected *Escherichia coli* β-galactosidase (β-gal) and maltose-binding protein (MBP) to the UPP for proteolytic removal.[22] Importantly, neither of the POIs are natural substrates for CHIP, and the degradation that we observed did not depend on the biological function or interaction partners of the POIs. Also noteworthy is the extremely modular architecture of uAbs: the interchange of synthetic binding proteins enables the generation of new uAbs that recognize completely different POIs,[26−34] while swapping E3 domains enables tailoring of the catalytic efficiency and/or E2 specificity.[27,34] It is even possible to deplete certain protein subpopulations (*e.g.*, active/inactive, post-translationally modified/unmodified, wild-type (wt)/mutant, *etc.*) while sparing others.[17,18,27]

Here, we exploited the versatility of uAbs to construct proteome editors capable of selectively removing the major isoforms of extracellular signal-regulated kinase (ERK), namely, ERK1 and ERK2, which share ∼85% identity and appear to be functionally equivalent.[35] Following activation by upstream kinases in the mitogen-activated protein kinase (MAPK) pathway that phosphorylate tyrosine and threonine residues,[36] ERK1/2 proceeds to phosphorylate numerous

https://doi.org/10.1021/acssynbio.1c00357
ACS Synth. Biol. 2021, 10, 2396−2408

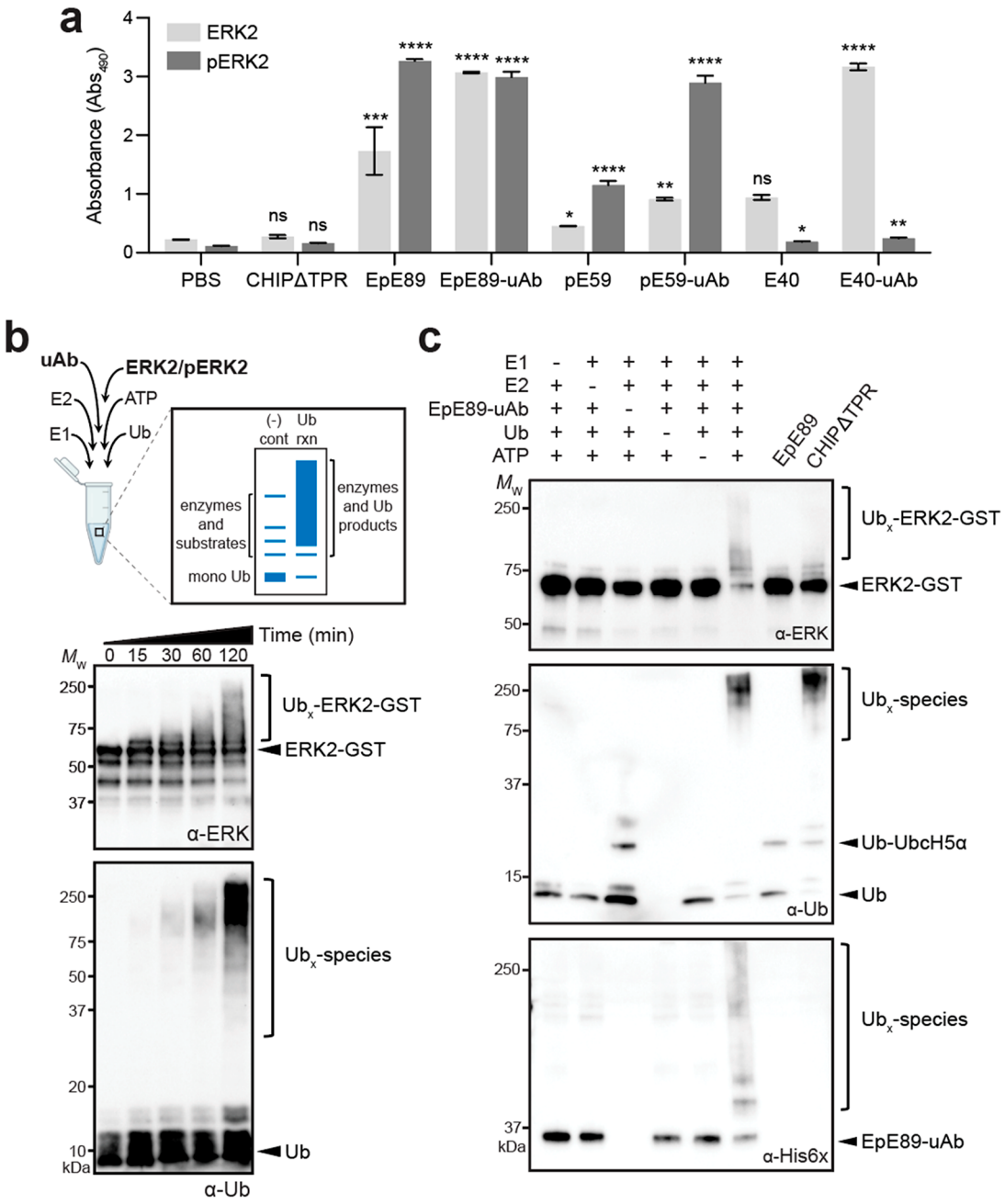

Figure 2. Engineered uAbs bind and ubiquitinate ERK *in vitro*. (a) ELISA of purified uAbs, DARPins, and CHIPΔTPR against immobilized ERK2 or pERK2 as indicated. Buffer only (PBS) served as a negative control. An equivalent amount of each uAb, DARPin, and CHIPΔTPR protein was used in the assay. Data are the average of three biological replicates, and error bars represent the standard deviation of the mean. p values were determined by the paired sample t test for all values relative to the PBS controls; ns, not significant; *, $p < 0.05$; **, $p < 0.01$; ***, $p < 0.001$; ****, $p < 0.0001$. (b) *In vitro* ubiquitination of nonphosphorylated ERK2 (ERK2−GST) in the presence of purified EpE89−uAb along with E1, E2, ubiquitin (Ub), and ATP. Samples were collected at the indicated times and subjected to immunoblotting. The figure was made using BioRender.com. (c) Same as in (b) but all reactions were run for 120 min in the presence (+) or absence (−) of each pathway component as indicated. Controls included EpE89 and CHIPΔTPR in the presence of all pathway components. For all blots, an equivalent amount of total protein was added to each lane. Immunoblots were probed with pan-ERK antibody (α-ERK) and anti-ubiquitin (α-Ub) to detect ERK2 and Ub species, respectively, and anti-His6x antibody to detect uAb. Bands corresponding to ERK2, Ub, EpE89−uAb, and polyubiquitinated species (Ub_x) are marked on the right. Molecular weight (M_W) markers are indicated on the left. Results are representative of at least three biological replicates.

downstream substrates that participate in vital physiological processes such as differentiation, proliferation, survival, and death.[37,38] We chose to focus on ERK1/2 because the MAPK pathway is the most frequently mutated signaling pathway in human cancer, making components of this cascade attractive targets for drug development.[36] To this end, a significant number of RAF and MEK inhibitors have been preclinically and clinically evaluated, which is in contrast to the more limited development of selective ERK1/2 inhibitors. While there are many reasons for this discrepancy,[36] occupancy-based inhibitors specific for ERK are very difficult to design due to the high homology between active-site pockets of ERK1/2 and cyclin-dependent kinases (CDKs).

https://doi.org/10.1021/acssynbio.1c00357
ACS Synth. Biol. 2021, 10, 2396−2408

To address this challenge, we generated a global ERK degrader by recombining human CHIP's discrete catalytic U-box domain with a pan-specific DARPin named EpE89 that recognizes both nonphosphorylated ERK1 and ERK2 as well as the doubly phosphorylated forms, pERK1 and pERK2.[39] Our results demonstrated the efficacy of this engineered uAb, as well as a second design based on a pERK1/2-specific DARPin named pE59,[39] in pan-selectively inducing ubiquitin-mediated degradation of all major ERK1/2 proteoforms in cultured cells. In addition, we uncovered the molecular basis for pan-specificity, which appeared to originate from an ability of the engineered uAbs to install polyubiquitin, including K-48-linked chains, on both ERK2 and pERK2.

RESULTS AND DISCUSSION

Construction of a Pan-Specific ERK Ubiquibody. Human CHIP is a U-box-type ubiquitin ligase composed of three distinct domains: a tetratricopeptide repeat (TPR) domain at the N-terminus, a U-box domain at the C-terminus, and a coiled-coil linker connecting the two (Figure 1a).[40,41] The TPR domain binds to the molecular chaperones Hsc70-Hsp70 and Hsp90, thereby promoting ubiquitin transfer onto chaperone client proteins.[42] To convert CHIP into a pan-specific ERK degrader, we replaced its N-terminal TPR domain with DARPin EpE89 that recognizes nonphosphorylated and doubly phosphorylated ERK1 and ERK2 (Figure 1a).[39] For comparison purposes, we constructed two additional uAbs composed of phospho-isoform-specific DARPin pE59, which preferentially binds pERK1 and pERK2, and DARPin E40, which specifically recognizes nonphosphorylated ERK1 and ERK2.[39] Our uAb designs retained the flexible coiled−coiled domain of CHIP, which has been shown to be critical for E3 dimerization,[40] as well as the catalytic U-box domain. A short linker of five amino acids (Gly−Ser−Gly−Ser−Gly) was included to ensure flexibility between the C-terminal capping helices of the DARPin and helix α7 of the N-terminally truncated CHIP (CHIPΔTPR) (Figure 1a,b). The rationally designed uAbs were expressed in the cytoplasm of *E. coli* cells and purified by Ni-NTA affinity chromatography, resulting in soluble titers (~30 mg of protein per liter of culture) that were notably higher than their unfused DARPin counterparts (Supplementary Figure 1a). This latter observation indicated that the CHIPΔTPR domain somehow enhanced the expression of its DARPin fusion partners. Following purification and characterization by size exclusion chromatography (SEC), the uAbs were observed to elute slightly earlier than the nonaggregated portion of wild-type CHIP (Supplementary Figure 1b). Since CHIP eluted at a volume expected of a dimer with a large water shell, consistent with the observation that the U-box of human CHIP functions as a homodimer,[40,41] we concluded that the uAbs were similarly assembled as dimeric structures akin to their parental E3 ubiquitin ligase.

Reprogramming the Substrate Specificity of CHIP with ERK-Binding DARPins. The extent to which CHIP's substrate specificity was switched by tethering to pan-ERK-specific EpE89 was first evaluated using a previously described affinity precipitation assay.[39] In this assay, lysate derived from human embryonic kidney (HEK) 293T cells, a common epithelial cell line, was incubated with purified EpE89−uAb, which was subsequently captured by Ni-NTA beads. Immunoblotting analysis revealed that EpE89−uAb was able to precipitate endogenous ERK1 and ERK2 as evidenced by the cross-reactivity of elution fractions with a phosphorylation state-independent anti-ERK antibody that recognizes all ERK isoforms including phosphorylated ones (Supplementary Figure 2a). Similar affinity precipitation was achieved with pE59−uAb, E40−uAb, and the unfused DARPins with the behavior of the latter in agreement with Kummer *et al.*[39] In contrast, CHIPΔTPR and the nonspecific control Off7−uAb, a chimera between CHIPΔTPR and the DARPin Off7 that binds the *E. coli* maltose-binding protein,[43] were unable to capture ERK1/2. Importantly, none of the proteins precipitated Hsp70, a native substrate of full-length CHIP,[42] indicating that CHIP's substrate specificity had been effectively reprogrammed by swapping the TPR domain with the ERK-binding DARPins.

To evaluate the pan-specificity of EpE89−uAb in more detail, we performed an enzyme-linked immunosorbent assay (ELISA) using ERK2 and pERK2 as immobilized antigens. Consistent with the known binding specificity of unfused EpE89,[39,44] the EpE89−uAb bound avidly to both ERK2 and pERK2. The pE59−uAb and E40−uAb constructs similarly mirrored the substrate preferences of their parental DARPins, specifically binding pERK2 and ERK2, respectively, at levels that rivaled the binding activity of pan-specific EpE89−uAb for each target (Figure 2a and Supplementary Figure 2b).

It should be noted that, while pE59−uAb and its unfused pE59 counterpart clearly preferred cognate pERK2, each bound to nonphosphorylated ERK2 at a low but statistically significant level above background. A similar pattern was observed for E40−uAb and E40 with each preferring ERK2 but showing a low but statistically significant level of binding to noncognate pERK2. These results are consistent with previous findings that the binding affinities between each of these DARPins and its noncognate ERK2 or pERK2 form, while significantly weaker than that with the cognate form, were still in the low micromolar range.[39] Importantly, there was no detectable binding activity between the N-terminally truncated CHIPΔTPR construct, which lacked a substrate-binding domain, and either ERK2 or pERK2 (Figure 2a and Supplementary Figure 2b). The enhanced binding measured for the dimeric uAbs relative to the unfused DARPins is likely due to an avidity effect, as the uAbs are dimers whereas DARPins are monomeric. Overall, these results indicate that the DARPins successfully reprogrammed CHIP specificity for distinct ERK forms with EpE89−uAb showing the clearest capacity for pan-specific ERK silencing.

Ubiquibodies Promote Ubiquitin Transfer to ERK. Having demonstrated that EpE89−uAb possessed pan-specific ERK binding, we next carried out *in vitro* ubiquitination assays using purified UPP components (E1, E2, ubiquitin, and ATP) along with EpE89−uAb as the E3 and ERK2 as the target. It should be noted that ERK2 has 24 potential ubiquitin attachment sites: 23 internal lysines as well as its N-terminus (Figure 2b). The E2 enzyme UbcH5α was chosen because of its demonstrated ability to function with CHIP *in vitro*.[22,45] Following *in vitro* reactions, we observed ubiquitinated ERK2, which appeared as high-molecular weight (HMW) bands in immunoblots probed with the pan-ERK antibody. These HMW ERK2 bands correlated with the appearance of HMW ubiquitin species that were detected with the anti-ubiquitin antibody (Figure 2b). The intensity of the HMW bands became more pronounced at later incubation times, which was characteristic of the polyubiquitination mediated by CHIP in the presence of native and non-native targets.[22,45] Similar

https://doi.org/10.1021/acssynbio.1c00357
ACS Synth. Biol. 2021, 10, 2396−2408

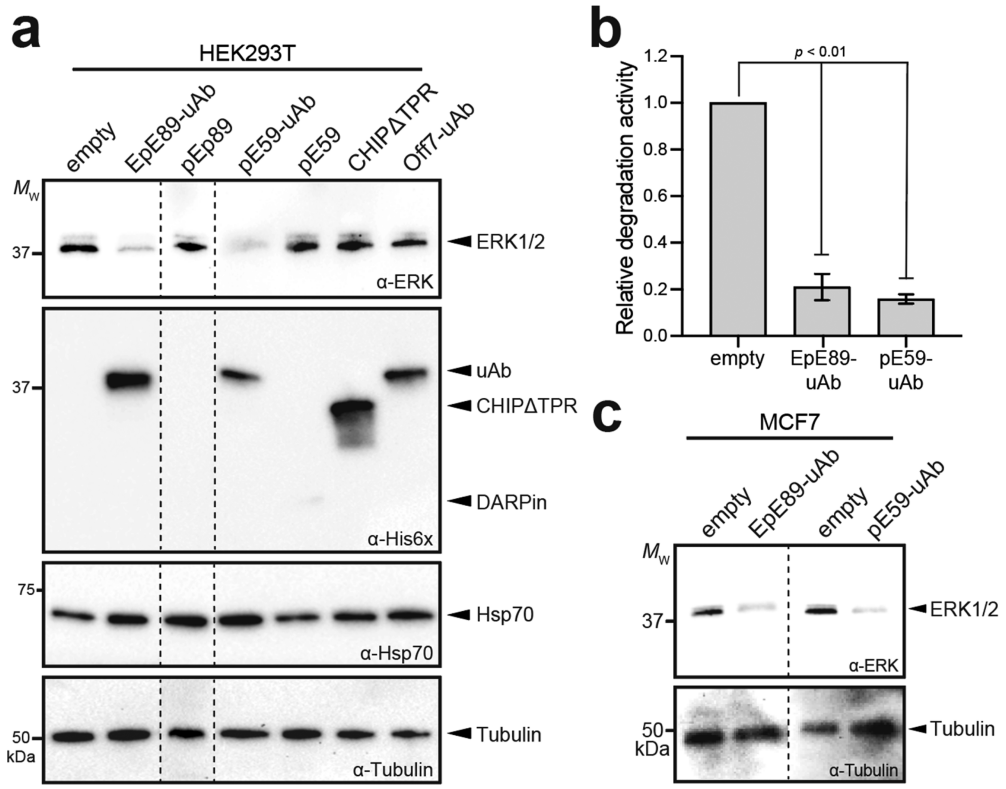

Figure 3. Engineered uAbs efficiently degrade endogenous ERK in living cells. (a) Immunoblot analysis of extracts prepared from HEK293T cells transfected with empty pcDNA3 or pcDNA3 encoding each of the constructs indicated at 0.25 μg of plasmid DNA per well. Cells were harvested 24 h post-transfection, after which extracts were prepared and subjected to immunoblotting. Blots were probed with the following: pan-ERK antibody (α-ERK) to detect total ERK1/2 expression; polyhistidine antibody (α-His6x) to detect uAbs, DARPins, and CHIPΔTPR constructs; Hsp70-specific antibody (α-Hsp70) to detect native CHIP substrate. Lanes were normalized by total protein content, and equivalent loading was confirmed by probing with β-tubulin (α-Tub). Molecular weight (M_W) markers are indicated on the left. Results are representative of at least three biological replicates. (b) Relative quantitation of total ERK1/2 levels by densitometry analysis of α-ERK immunoblot images using ImageJ software. Intensity data for uAb bands was normalized to band intensity for empty plasmid control cases from six independent experiments. Error bars represent the standard deviation of the mean. p values were determined by a paired sample t test. (c) Immunoblot analysis of extracts prepared from MCF7 cells transfected with empty pcDNA3 or pcDNA3 encoding EpE89−uAb or pE59−uAb at 0.25 μg of plasmid DNA per well. Blots prepared as in (a). The dashed line indicates splicing of the same blot.

ubiquitination results were observed for pE59−uAb and E40−uAb (Supplementary Figure 2c). Only in reactions where all UPP components were included was ubiquitination observed, whereas none of the controls (unfused binding domain, unfused EpE89, or unfused CHIPΔTPR) were capable of producing ubiquitinated ERK2 (Figure 2c). Collectively, these results confirm that the catalytic activity of the truncated CHIPΔTPR domain was preserved in the chimeric uAb format, leading to the efficient transfer of ubiquition to the non-native ERK2 target.

Ubiquibodies Efficiently Degrade Exogenous and Endogenous ERK. To characterize the degradation potential of pan-ERK-specific EpE89−uAb, we first evaluated the soluble expression in mammalian cells. Specifically, wild-type (wt) HEK293T cells were transiently transfected with plasmid DNA encoding the chimeric EpE89−uAb construct, and cell lysate was prepared 24 h post-transfection. The strong expression of EpE89−uAb was detected in soluble lysates by immunoblot analysis using an anti-His6x antibody (Supplementary Figure 3a). Interestingly, while pE59−uAb also exhibited a strong soluble expression, the E40−uAb construct was barely detectable. To determine whether this poor expression was somehow related to the cell line, we also expressed the uAbs in MCF7 breast cancer cells and observed an identical expression pattern (Supplementary Figure 3b). In light of these poor steady-state levels observed for E40−uAb, we focused our attention on the EpE89−uAb and pE59−uAb constructs hereafter. It is also worth mentioning that the expression of the three unfused DARPins was barely detectable under the conditions tested (Supplementary Figure 3b), providing additional evidence for the ability of the CHIPΔTPR domain to enhance the soluble expression and revealing an unexpected benefit arising from uAb chimeragenesis.

To investigate the intracellular knockdown, we next leveraged an exogenously expressed ERK2−EGFP reporter fusion. Specifically, a previously engineered cell line that stably expresses an ERK2−EGFP−encoding transgene (HEK293-$T^{ERK2-EGFP}$)[27] was transiently transfected with plasmid DNA encoding the uAbs. Immunoblot analysis of lysate derived from these cells revealed that the expression of both EpE89−uAb and pE59−uAb promoted efficient clearance of ERK2−EGFP relative to the steady-state level observed in the same cells transfected with an empty plasmid or plasmid DNA encoding either CHIPΔTPR or Off7−uAb (Supplementary Figure 3c). The depletion of ERK2−EGFP protein levels by EpE89−uAb and pE59−uAb coincided with an overall reduction of GFP fluorescence as determined by flow cytometric analysis (Supplementary Figure 3c). The extent of fluorescence

https://doi.org/10.1021/acssynbio.1c00357
ACS Synth. Biol. 2021, 10, 2396−2408

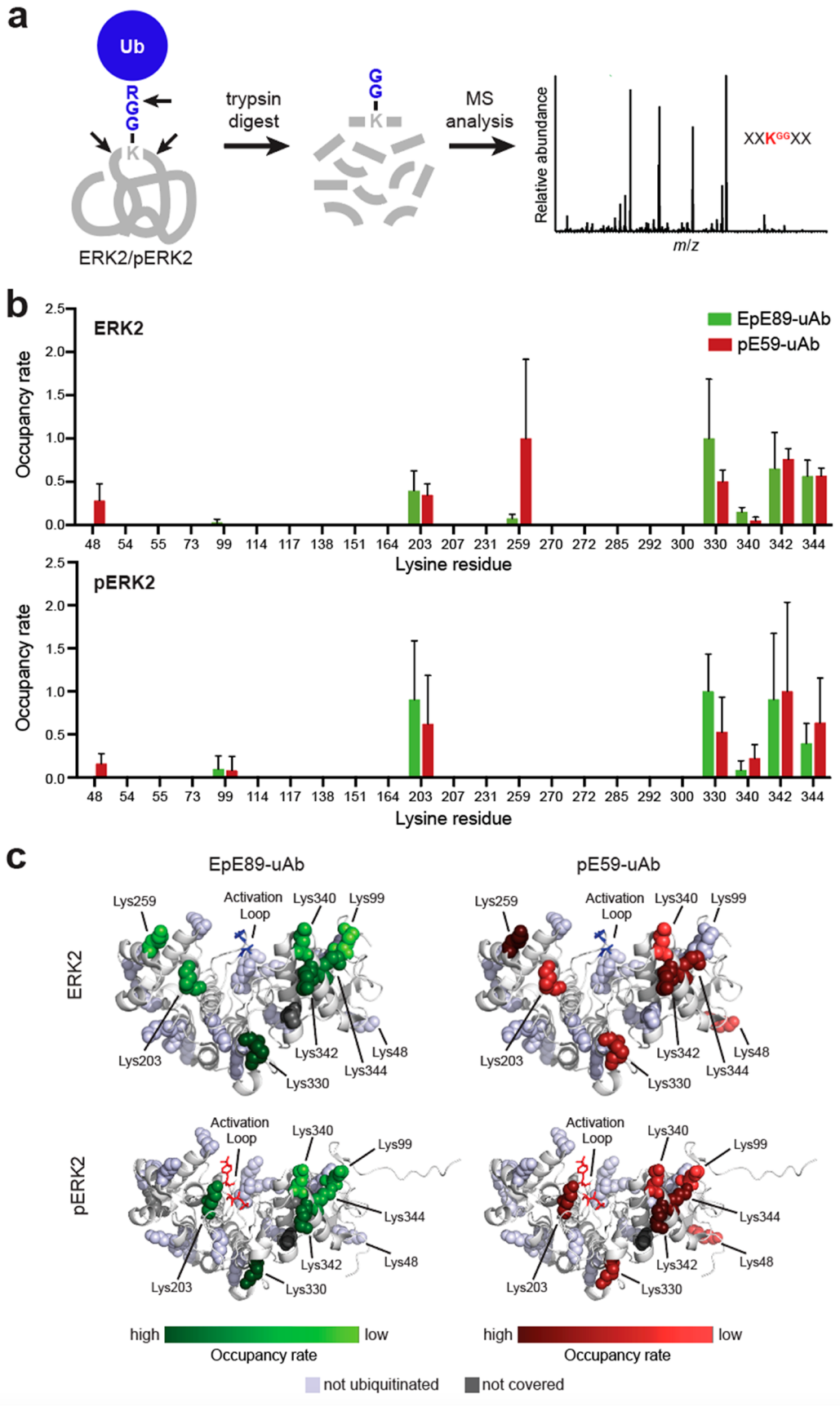

Figure 4. Engineered uAbs install ubiquitin on multiple lysine residues in ERK2 and pERK2. (a) Schematic of the ubiquitin profiling experiment for revealing precise ubiquitination sites in ERK2/pERK2. Briefly, mass spectrometry can be used to identify ubiquitin attachment sites based on the characteristic mass shift caused by the presence of diglycine (GG) that is retained on ubiquitinated lysine residues within peptides after trypsin digestion. (b) Occupancy rate of GG modification of ERK2/pERK2 lysine residues by EpE89−uAb and pE59−uAb by LC-MS/MS. Peptides

https://doi.org/10.1021/acssynbio.1c00357
ACS Synth. Biol. 2021, 10, 2396−2408

Figure 4. continued

corresponding to 80% of the ERK2/pERK2 sequences were identified using Mascot software. Data were generated by normalizing ubiquitinated residue counts relative to total residue counts and by averaging across three independent experiments. Ubiquitinated peptide counts of peptides containing more than one non-C-terminal lysine residue were averaged over all non-C-terminal lysines. (c) Mapping of ubiquitination sites on ERK2 and pERK2 where ERK2/pERK2 backbones are shown as white ribbons and ubiquitinated lysines represented as spheres colored by the heat map as indicated. Lysines not covered by mass spectrometry analysis (dark gray spheres) and lysines not identified as ubiquitinated (light gray spheres) are also depicted. Structures adapted from PDB ID: 3ZU7 (ERK2) and PDB ID: 3ZUV (pERK2) of Kummer *et al.*[39] using PyMOL software.

reduction associated with the ERK2−GFP knockdown was reminiscent of that observed previously for EGFP−HRAS, EGFP−KRAS, and SHP2−EGFP using uAbs composed of synthetic binding proteins against HRAS, KRAS, and SHP2, respectively.[27]

While the above results demonstrated the feasibility for the uAb-mediated knockdown of an ERK2-containing fusion protein in living cells, we cannot rule out the possibility that ubiquitin was conjugated exclusively to the EGFP domain and not to ERK1/2, which would limit the practical utility of EpE89−uAb and pE59−uAb for proteolytic silencing of untagged ERK forms. Interestingly, the pan-specific ERK antibody used to detect ERK2−EGFP also revealed the depletion of endogenous ERK proteins in the lysates derived from cells expressing EpE89−uAb and pE59−uAb (Supplementary Figure 3c), suggesting that the uAbs could indeed accelerate the turnover of unmodified ERK in addition to its EGFP-tagged counterpart. However, even this result was inconclusive as endogenous ERK1 and ERK2 are known to homodimerize,[46] which leaves open the possibility that endogenous ERK2 could heteroassemble with ubiquitinated ERK2−EGFP (where again the ubiquitin might be installed on EGFP only) and become targeted for proteolysis *via* a piggyback mechanism.

Therefore, we focused our attention on determining the extent to which endogenously expressed, unmodified ERK could be degraded by EpE89−uAb and pE59−uAb. To this end, wt HEK293T cells were transiently transfected with the EpE89−uAb and pE59−uAb-encoding plasmids. After 24 h, transfected cells displayed dramatically reduced steady-state levels of total ERK1/2 compared to cells receiving empty plasmid DNA as detected by the phosphorylation-insensitive pan-ERK antibody (Figure 3a,b). Because cytoplasmic ERK is present as a mixture of nonphosphorylated and phosphorylated forms in both nonstimulated and stimulated HEK293T cells,[39,47] we also probed lysates with an anti-pERK1/2 antibody. Consistent with their strong pERK2 binding activity, both uAbs showed a potent reduction of pERK levels that mirrored total ERK knockdown with pE59−uAb promoting a greater reduction of pERK (Supplementary Figure 4). Importantly, the transfection of HEK293T cells with unfused EpE89, pE59, or CHIPΔTPR resulted in little to no change in total ERK1/2 protein levels, indicating that none of these domains alone was capable of target depletion and confirming the importance of the bifunctional uAb design. The nonspecific Off7−uAb was also incapable of promoting ERK1/2 degradation, thereby validating the targeted nature of ERK depletion by EpE89−uAb and pE59−uAb. As was seen above, the soluble expression of the DARPins was greatly enhanced by fusion to CHIPΔTPR. It is also noteworthy that the levels of a housekeeping protein, β-tubulin, and the native CHIP substrate, Hsp70, were not affected by the expression of EpE89−uAb, pE59−uAb, or any of the other control constructs.

We next explored whether our anti-ERK approach would work in other cell lines. Specifically, we investigated the ability of EpE89−uAb and pE59−uAb to degrade ERK in MCF7 breast cancer cells, which have served as a useful model for studying ERK expression, activation, and signaling.[48,49] Akin to the results with HEK293T, we observed a strong reduction of total ERK1/2 levels in MCF7 cells transfected with plasmid DNA encoding the EpE89−uAb and pE59−uAb constructs compared to cells transfected with empty plasmid (Figure 3c). Degradation was most pronounced at 24 h post-transfection; however, clearly visible depletion of ERK1/2 persisted for 48 and 72 h (Supplementary Figure 3b), consistent with the duration of the uAb-mediated GFP silencing observed in our previous work.[27]

Pan-Specific uAbs Transfer Ubiquitin to Distinct Sites on ERK and pERK. To further elucidate the origins of pan-specific degradation, we profiled the ubiquitination patterns generated by EpE89−uAb and pE59−uAb on nonphosphorylated and phosphorylated ERK2. Specifically, *in vitro* ubiquitination reactions were performed with each of the uAbs in the presence of either ERK2 or pERK2 as substrates, after which HMW products (∼50−250 kDa) were resolved by SDS-PAGE, excised from the gel, digested with trypsin, and analyzed by liquid chromatography-tandem mass spectrometry (LC-MS/MS; Figure 4a). When a ubiquitinated protein is subjected to tryptic digestion, a C-terminal glycine−glycine dipeptide derived from ubiquitin remains attached to the ubiquitinated lysine residue.[50] Therefore, the MS data was thoroughly scanned for this modification on the ERK2/pERK2 peptides and the identified Lys residues to which ubiquitin was conjugated. In general, the ubiquitination profiles of EpE89−uAb and pE59−uAb were highly similar with both uAbs transferring ubiquitin to multiple lysine residues in ERK2 and pERK2 (Figure 4b). These overlapping profiles help to explain the observed pan-specific ERK degradation of each uAb. Moreover, both uAbs preferentially ubiquitinated one face of ERK2/pERK2 (oriented forward in Figure 4c), consisting of the plane formed by the N- and C-lobes near the active site of ERK2. This face was aligned with the positioning of the C-terminus of the DARPins with ERK2 as seen in cocrystal structures[39] and would thus be located in the closest proximity to CHIPΔTPR when bound by the uAb chimera (Figure 1b).

Of the 23 total lysines in ERK2, 7 sites (K48, K99, K203, K330, K340, K342, and K344) were found to be modified in both ERK2 and pERK2 (Figure 4b,c). Only one additional residue, K259, was ubiquitinated in ERK2 and not pERK2, suggesting that the conformational change upon phosphorylation may reposition K259 away from the U-box-bound, ubiquitin-charged E2, UbcH5α. This site was also interesting because it was much more frequently modified by pE59−uAb than EpE89−uAb in ERK2 and was not modified by either

https://doi.org/10.1021/acssynbio.1c00357
ACS Synth. Biol. 2021, 10, 2396−2408

uAb in pERK2. Four of the modified lysine residues (K99, K340, K342, and K344) were clustered in the three-dimensional structure of ERK2 (Figure 4c), providing clues about the orientation of the charged E2−uAb complex relative to the target surface and consistent with the predicted plane of ubiquitination (Figure 1b). Residues K203 and K330 were among the most frequently ubiquitinated despite being positioned away from the plane of ubiquitination, suggesting mobility of the E2−uAb complex as has been observed previously for native E2−E3 complexes.[51] Residue K48 was one of the least often ubiquitinated sites and the only lysine not on the same face of ERK to be ubiquitinated. Interestingly, K48 in both ERK2 and pERK2 was modified by EpE89−uAb but not at all by pE59−uAb, suggesting that the DARPin domains recognize different epitopes and thus position the uAbs in different orientations relative to ERK2/pERK2, which subsequently affects how ubiquitin is attached to the substrate.

The polyubiquitin chain topology formed by the uAbs was analyzed using an identical LC-MS/MS approach that identified C-terminal glycine−glycine dipeptides on ERK2-conjugated ubiquitin molecules (Supplementary Figure 5a). According to this analysis, both uAbs produced nearly identical ubiquitin chain topologies, preferentially forming K6, K11, K48, and K63 polyubiquitin linkages in the presence of E2 UbcH5α (Supplementary Figure 5b). Identical linkage patterns were observed previously on native and non-native substrates that had been subjected to *in vitro* ubiquitination in the presence of wild-type CHIP or CHIP-based uAbs.[22,52] These results are significant from a targeted degradation standpoint, as K48 serves as the predominat recognition signal for the 26S proteasome and commonly promotes substrate degradation,[7] while K6, K11, and K63 have also been implicated as proteasomal targeting signals.[53,54] Taken together, these results provide clear evidence for highly similar ERK2/pERK2 ubiquitination by EpE89−uAb and pE59−uAb, thereby providing a convenient explanation for their comparable pan-specific ERK degradation.

Altogether, we engineered chimeric uAbs composed of the human E3 ubiquitin ligase CHIP and different ERK-specific DARPins that were capable of accelerating the turnover of exogenous or endogenous ERK protein kinase. In particular, two of the uAbs were shown to be global ERK degraders, redirecting all ERK1/2 proteoforms, including both active (doubly phosphorylated) and inactive (nonphosphorylated) conformations, to the 26S proteasome for degradation in different cell lines including MCF7 breast cancer cells. These results add to a growing body of evidence that reveals the effectiveness of designer uAb constructs in promoting the clearance of POIs,[22,26−34] including some that have been classified as difficult-to-drug.

CONCLUSION

Ubiquibodies are a customizable proteome editing technology for inducing targeted proteolysis of intracellular proteins and thus hold great potential as both a research tool for dissecting protein networks and a therapeutic modality with the potential for inhibiting drug targets that have so far evaded pharmacological intervention. As we demonstrated here and in previous works, the combination of synthetic binding proteins having affinity and specificity for the POI with the catalytic domain of E3 ligases opens the door to targeted knockout of intracellular proteins and their post-translationally modified isoforms. Indeed, uAb technology has been used to degrade numerous structurally diverse POIs that span a broad range of molecular weights and subcellular locations including the cytoplasm, nucleus, and cell membrane.[18−22,27] Importantly, the design and construction of uAbs are not dependent on the biological function or interaction partners of the POI. Instead, uAbs take advantage of synthetic binding proteins that have already been developed or that emerge anew such as from ambitious campaigns to develop *de novo* protein binders on a human proteome-wide scale.[25] Because the generation of antibodies or nonantibody scaffolds that bind to a target with high specificity and affinity is generally easier than the generation of small molecules that do the same, the ability to rapidly prototype bespoke degraders against new and emerging targets should be more tractable with uAbs than with PROTACs.[3,55]

Another key consideration for the deployment of uAbs is their overall silencing efficiency, which will depend on a number of factors including the intracellular uAb expression level as well as the expression level of the POI. With respect to the former, while we have not quantified the dosage of uAb needed to achieve the high levels of endogenous ERK depletion (>80%) observed here, one unexpected advantage of using the human CHIPΔTPR domain was its ability to enhance the soluble expression of the synthetic target-binding protein to which it was fused, thereby ensuring reasonably high intracellular uAb concentrations in most contexts. On the topic of target protein level, this is also an important variable that will directly impact the success of targeted degradation efforts. In the case of endogenous ERK, it has been reported that there are 75−170 × 10^4 ERK molecules per cell with the exact number depending on the specific cell line.[56] This range is quite a bit higher than other MAP kinases such as Ras, Raf-1, and MEK-1, which are present endogenously in the range of 1−36 × 10^4 molecules per cell[56] and thus bodes well for future campaigns to develop uAbs against these other important cancer targets. It is also worth mentioning that uAbs can deplete even higher levels of intracellular proteins as evidenced by the ability of pEpE89−uAb and pE59−uAb to efficiently degrade ERK2−EGFP that was expressed from a transiently transfected DNA plasmid. Indeed, the ERK2−EGFP target in this experiment was expressed at levels that were significantly higher than the endogenous levels of ERK1/2 as seen in anti-ERK immunoblots (Supplementary Figure 3c). These results were reminiscent of the efficient silencing that we have observed for other highly expressed, plasmid-encoded targets.[22,27]

The depletion of total ERK pools obtained with EpE89−uAb was expected given its affinity for both ERK and pERK; however, the ability of pE59−uAb to also function as a pan-specific degrader was somewhat surprising given its reported specificity for pERK.[39] We suspect that, despite its clear preference for pERK, pE59−uAb may bind noncognate ERK2 with enough affinity to still promote efficient substrate turnover. Indeed, the unfused pE59 DARPin is known to bind noncognate ERK2 with micromolar affinity (K_D = 3.5−8.7 μM[39]), which should be sufficient to promote ubiquitin transfer given that the measured affinity between CHIP and its native substrates Hsp70, Hsp90, and Hsc70 is also in the low micromolar range (K_D = 0.3−2.3 μM).[57] Moreover, the binding of ERK2 by pE59−uAb is likely to be enhanced by avidity effects that arise from dimerization of the CHIP-based uAb. Importantly, while pan-specific degraders were generated here that promoted the degradation of multiple proteoforms,

https://doi.org/10.1021/acssynbio.1c00357
ACS Synth. Biol. 2021, 10, 2396−2408

uAbs have also been created that selectively degrade distinct forms of a protein.[17,18,27] Collectively, the designer binding of uAbs could open up new avenues for therapeutically targeting proteins that are dysregulated in a diseased state by either degrading an entire family of functionally overlapping proteins or preferentially ablating a specific post-translationally modified protein. In the case of ERK, it has been proposed that ERK1/2-selective inhibitors could offer a therapeutic benefit in a range of human malignancies bearing mutations in RAS, RAF, and MEK.[36,58] Given the functional redundancy of ERK1 and ERK2, the broad inactivation of both family members may be needed to inhibit cellular proliferation, cause apoptosis in tumor cells, and induce significant tumor regression, a hypothesis that could be investigated using our pan-ERK-specific degraders. To this end, it should be pointed out that promising *in vivo* results have been obtained using experimental viral and nonviral vectors to deliver uAb genes,[20,27,59,60] indicating that clinical translation may not be that far off.

MATERIAL AND METHODS

Plasmid Construction. *E. coli* strain DH5α was used for the construction and propagation of all plasmids. Plasmids encoding the uAb constructs and the related controls were generated following published protocols.[34] Genes encoding each of the DARPins were PCR amplified from pDST67-based plasmids encoding EpE89, pE59, and E40[39] using primers that introduced NcoI and *Eco*RI overhangs. The resulting PCR amplicons were ligated in plasmid pET28a−R4−uAb,[22] which had been doubly digested with NcoI/*Eco*RI to excise the gene encoding scFv13−R4 (R4). This process yielded plasmids pET28a−EpE89−uAb, pET28a−pE59−uAb, and pET28a−E40−uAb, which encoded each of the DARPins followed by a flexible GSGSG linker and then CHIPΔTPR bearing a tandem FLAG-His6x sequence at its C-terminus. A similar strategy was used to generate plasmid pET28a−Off7−uAb, where the gene encoding Off7 was PCR amplified from plasmid pRH−DsbA−Off7[61] (a kind gift from Mark Ostermeier, Johns Hopkins University). To generate plasmid pET28a−CHIPΔTPR for the expression of unfused CHIPΔTPR, a gene fragment corresponding to amino acids 128−303 of human CHIP was PCR amplified with primers that introduced NcoI and *Sal*I overhangs and ligated into the same sites in plasmid pET28a−R4−uAb that had been doubly digested with NcoI/*Sal*I to excise the R4−uAb while leaving behind the tandem FLAG-His6x sequence. To generate plasmids for expression of unfused DARPins, genes encoding each of the DARPins were similarly PCR amplified from pDST67-based plasmids using primers that introduced NcoI and *Hin*dIII overhangs as well as an N-terminal RGS-His6x sequence. The resulting PCR amplicons were cloned into pET28a(+) between NcoI and *Hin*dIII, yielding plasmids pET28a−EpE89, pET28a−pE59, and pET28a−E40. For expression in human cell lines, all uAbs and control proteins were cloned into plasmid pcDNA3, a mammalian expression vector with constitutive CMV promoter. This involved PCR amplification of the target genes using the respective pET28a-based vectors described above as template along with primers that introduced *Hin*dIII and XbaI overhangs and a Kozak sequence at the start codon. The resulting PCR amplicons were then ligated between the *Hin*dIII and XbaI sites in pcDNA3 to yield the desired plasmids including pcDNA3−EpE89−uAb, pcDNA3−pE59−uAb, and pcDNA3−E40−uAb. All plasmids were confirmed by DNA sequencing at the Biotechnology Resource Center (BRC) Genomics Facility at the Cornell Institute of Biotechnology.

Protein Expression and Purification. All purified uAbs, unfused DARPins, and CHIPΔTPR were obtained from cultures of *E. coli* BL21(DE3) cells carrying pET28a-based vectors grown in Luria−Bertani (LB) medium. The expression was induced with 0.1 mM IPTG when the culture density (Abs_{600}) reached 0.6−0.8 and proceeded for 6 h at 30 °C, after which cells were harvested by centrifugation at 4000*g* for 20 min at 4 °C. The resulting pellets were stored at −80 °C overnight. Thawed pellets were resuspended in 15 mL of phosphate-buffered saline (PBS) supplemented with 10 mM imidazole (pH 7.4) and lysed with a high-pressure homogenizer (Avestin EmulsiFlex-C5). Lysates were cleared of insoluble material by centrifugation at 20 000*g* for 20 min at 4 °C. Clarified lysates containing His6x-tagged proteins were subjected to gravity-flow Ni^{2+}-affinity purification using HisPur Ni-NTA resin (ThermoFisher) following the manufacturer's protocols. Elution fractions were desalted into PBS buffer (pH 7.4) using PD-10 desalting columns (Cytiva) following the manufacturer's protocols. Purified proteins were stored at 4 °C for up to 2 weeks or diluted to 25% (v/v) glycerol and stored indefinitely at −80 °C. The final purity of all proteins was confirmed by SDS-polyacrylamide gel electrophoresis (PAGE) and Coomassie staining. The purity of all proteins was typically >95%.

Purified uAbs and CHIPΔTPR were subjected to SEC analysis as described previously.[62] Standards used to calibrate the SEC column were a lyophilized mix of thyroglobulin, bovine γ-globulin, chicken ovalbumin, equine myoglobin, and vitamin B12 with MWs of 1350−670 000 and p*I*'s of 4.5−6.9 (BioRad). Proteins were stored at a final concentration of 1 mg/mL in SEC buffer (20 mM Tris, pH 7.5, 50 mM NaCl, 1 mM EDTA, pH 8.0) at 4 °C.

To produce biotinylated ERK2 and pERK2 proteins, strain BL21(DE3) was co-transformed with plasmid pSPI03-BirA-His[63] (a kind gift from Amy Karlsson, University of Maryland) along with either plasmid pLV-ERK2-Avi for expressing nonphosphorylated ERK2 or pLV-MEK1R4F-ERK2-His-Avi for expressing doubly phosphorylated ERK2, respectively.[39] These latter plasmids introduced N-terminal Avi tags on ERK2 and pERK2 for biotinylation *in vivo* by the biotin ligase BirA encoded in plasmid pSPI03-BirA-His and C-terminal His6x tags for affinity purification and immunodetection. Following the expression, bacterial cell pellets were harvested by centrifugation, pelleted, and resuspended in PBS (pH 7.4) with 1 mM DTT and 0.05% Tween 20. The resulting cell suspensions were homogenized as above, after which the clarified lysates containing biotinylated ERK2 and pERK2 were subjected to avidin agarose (ThermoFisher) to purify the Avi-tagged proteins according to the manufacturer's protocols. Following elution with 2 mM biotin, the eluents were subjected to Ni^{2+}-affinity purification as above to remove free biotin and further enhance the purity. Biotinylated ERK2 and pERK2 were analyzed by SDS-PAGE followed by Coomassie staining to confirm the purity, which was typically >95% for both proteins.

Affinity Precipitation. Affinity purification was performed as described.[64] Briefly, purified uAbs, unfused DARPins, and CHIPΔTPR were captured on HisPur Ni-NTA resin (ThermoFisher) by incubating 300 μg of each protein with 1 mL of resin slurry for 30 min at 4 °C with end-over-end

https://doi.org/10.1021/acssynbio.1c00357
ACS Synth. Biol. 2021, 10, 2396−2408

rotation. Prepared resin was incubated with 10 μL of lysate at 4 °C overnight. Resin was washed with PBS supplemented with 25 mM imidazole (pH 7.4), and proteins were eluted with PBS supplemented with 250 mM imidazole (pH 7.4). Samples were boiled with 2× Laemmli loading buffer and analyzed by immunoblotting as described below.

Protein Analysis. Proteins were separated using Precise Tris-HEPES 4−20% SDS-polyacrylamide gels (ThermoFisher). Coomassie R-250 stain (BioRad) was used to visualize proteins in SDS-PAGE. Immunoblotting was performed according to standard protocols. Following the transfer of proteins, the poly(vinylidene fluoride) (PVDF) membranes were probed with the following antibodies at a 1/2500 or 1/5000 dilution: rabbit anti-p44/42 MAPK (ERK1/2) antibody (Cell Signaling, cat # 4695 S) to detect ERK2; rabbit anti-p-p44/42 MAPK (ERK1/2) (Cell Signaling, cat # 9101 S) to detect pERK2; mouse anti-ubiquitin (Millipore, cat # P4D1-A11) to detect ubiquitin; rabbit anti-Lys27 (Abcam, cat # ab238442) to detect K27-linked ubiquitin; rabbit anti-Lys48 (Millipore, cat # Apu2) to detect K48-linked ubiquitin; rabbit anti-Lys63 (Millipore, cat # Apu3) to detect K48-linked ubiquitin; mouse anti-Hsp70 (Enzo Life Sciences, cat # C92F3A) to detect Hsp70; rabbit anti-β-tubulin (Cell Signaling Technology, cat # 5346) to detect β-tubulin; rabbit anti-FLAG-HRP (Abcam, cat # ab49763) to detect uAbs and CHIPΔTPR; rabbit anti-His6-HRP (Abcam; cat # ab1187) to detect uAbs, unfused DARPins, and CHIPΔTPR. Densitometry analysis of protein bands in immunoblots was performed using ImageJ software as described here: https://imagej.nih.gov/ij/docs/examples/dot-blot/. Briefly, bands in each lane were grouped as a row or a horizontal "lane" and quantified using ImageJ's gel analysis function. Intensity data for the uAb bands was normalized to band intensity for empty plasmid control cases from six independent experiments.

ELISA. To analyze binding to purified ERK and pERK, ELISA analysis was performed as described previously.[39] Briefly, biotinylated ERK2 and pERK2 (100 nM) were immobilized on NeutrAvidin-coated 96-well plates (Pierce) overnight at 4 °C and then washed twice with PBS (pH 7.4) supplemented with 1 mM DTT and 0.05% Tween 20. Next, the plates were blocked for 1 h with PBS (pH 7.4) supplemented with 1 mM DTT, 0.05% Tween 20, and 1% (w/v) BSA. All subsequent ELISA steps were performed at 4 °C in PBS (pH 7.4) with 1 mM DTT and 0.05% Tween 20. To measure binding activity, varying concentrations of purified uAbs, unfused DARPins, or CHIPΔTPR were applied to wells with or without ERK2 or pERK2 for 1 h. Following three washes, the binding activity was detected by rabbit anti-His6-HRP (Abcam; cat # ab1187) or mouse anti-RGS-His antibody (Qiagen; cat # 34610) at a 1:5000 dilution followed by goat antirabbit−HRP conjugate (Abcam; ab6789) at a 1:2500 dilution. After 1 h of incubation at room temperature, plates were washed and then incubated with SigmaFast OPD HRP substrate (Sigma) for 30 min in the dark. The reaction was quenched with 3 M H_2SO_4, and the absorbance of the wells was measured at 492 nm.

Ubiquitination Assays. Ubiquitination assays were performed as previously described[45] in the presence of 0.1 μM purified human UBE1 (Boston Biochem), 4 μM human UbcH5α/UBE2D1 (Boston Biochem), 3 μM uAb (or equivalent control protein), 1.5 μM human ERK2 or phosphoERK2 (ProQinase), 50 μM human ubiquitin (Boston Biochem), 4 mM ATP, and 1 mM DTT in 20 mM MOPs, 100 mM KCl, 5 mM $MgCl_2$, pH 7.2. Reactions were carried out at 37 °C for 2 h (unless otherwise noted) and stopped by boiling in 2× Laemmli loading buffer for analysis by immunoblotting.

Flow Cytometric Analysis. Cells were passed into 12-well plates at 10 000 cells/cm^2. At 16−24 h after seeding, cells were transiently transfected as described above. Culture media were replaced 4−6 h post-transfection. Then, 24 h post-transfection, cells were harvested and resuspended in PBS for analysis using a FACSCalibur (BD Biosciences). FlowJo software (Version 10) was used to analyze samples by geometric mean fluorescence determined from 10 000 events.

Cell Culture, Transfection, and Lysate Preparation. HEK293T and MCF7 cell lines were obtained from ATCC, while the HEK293T$^{ERK2-EGFP}$ cell line was previously generated in-house.[27] HEK293T and HEK293T$^{ERK2-EGFP}$ cells were cultured in DMEM media supplemented with high glucose and L-glutamine (VWR) supplemented with 10% Hyclone FetalClone I serum (VWR) and 1% penicillin−streptomycin−amphotericin B (ThermoFisher). MCF7 cells were cultured similarly, but insulin (10 mg/mL, Sigma) was added to the media. All cells were maintained at 37 °C, 5% CO_2, and 90% relative humidity (RH). Additionally, all cell lines were maintained at low passage numbers and routinely checked for *Mycoplasma* by PCR according to standard procedures. Cells were transfected in 6-well dishes at 60−80% confluency with 2 μg of total plasmid DNA using empty pcDNA3 plasmid to balance all transfections. Transfection was performed using jetPRIME (Polyplus Transfection) according to the manufacturer's instructions with a 1:2 ratio (w/v) of jetPRIME to DNA with growth media refreshed at 4 h post-transfection. At 24 h post-transfection, cell lysate was prepared by harvesting cells in PBS, pelleting at 8000*g* for 5 min at 4 °C, and freezing at −20 °C until analyzed by immunoblotting. Thawed pellets were lysed in NP40 lysis buffer (150 mM NaCl, 1% Nonidet P-40, 50 mM Tris-HCl, pH 7.4) by pipetting and mixing for 30 min at 4 °C. Soluble fractions were obtained by centrifugation of lysed cells at 18 000*g* for 20 min at 4 °C. Samples were boiled in 2× Laemmli sample buffer for analysis by immunoblotting.

Mass Spectrometry Analysis. For LC-MS/MS sample preparation, ubiquitination assays were performed as described above. Reactions were resolved by SDS-PAGE and stained by Coomassie R250 prior to gel excision. The protein bands were excised from an SDS-PAGE gel, cut into ∼1 mm^3 cubes, and submitted to the Biotechnology Resource Center (BRC) Proteomics and Metabolomics Facility at the Cornell Institute of Biotechnology for further analysis. Specifically, the gel bands were washed in 200 μL of deionized water for 5 min, followed by 200 μL of 100 mM ammonium bicarbonate/acetonitrile (1:1) for 10 min, and finally 200 μL of acetonitrile for 5 min. The acetonitrile was discarded, and the gel bands were dried in a speed-vac for 10 min. The gel pieces were rehydrated with 70 μL of 10 mM DTT in 100 mM ammonium bicarbonate and incubated for 1 h at 56 °C. The samples were allowed to cool to room temperature, after which 100 μL of 55 mM iodoacetamide in 100 mM ammonium bicarbonate was added, and the samples were incubated at room temperature in the dark for 60 min. Following incubation, the gel slices were again washed as described above. The gel slices were dried and rehydrated with 50 μL of trypsin at 50 ng/μL in 45 mM ammonium bicarbonate and 10% acetonitrile on ice for 30 min. The gel pieces were covered with an additional 25 μL of 45 mM ammonium bicarbonate and 10% acetonitrile and

https://doi.org/10.1021/acssynbio.1c00357
ACS Synth. Biol. 2021, 10, 2396−2408

incubated at 37 °C for 19 h. The digested peptides were extracted twice with 70 μL of 50% acetonitrile, 5% formic acid (vortexed 30 min and sonicated 10 min) and once with 70 μL of 90% acetonitrile, 5% formic acid. Extracts from each sample were combined and lyophilized.

The lyophilized in-gel tryptic digest samples were reconstituted in 20 μL of nanopure water with 0.5% formic acid for nanoLC-ESI-MS/MS analysis, which was carried out by a LTQOrbitrap Velos mass spectrometer (ThermoFisher) equipped with a CorConneX nano ion source device (CorSolutions LLC). The Orbitrap was interfaced with a nano HPLC carried out by an UltiMate3000 UPLC system (Dionex). The gel extracted peptide samples (2−4 μL) were injected onto a PepMap C18 trap column-nano Viper (5 μm, 100 μm × 2 cm, Thermo Dionex) at a 20 μL/min flow rate for online desalting and then separated on a PepMap C18 RP nanocolumn (3 μm, 75 μm × 15 cm, Thermo Dionex), which was installed in the "Plug and Play" device with a 10 μm spray emitter (New Objective). The peptides were then eluted with a 90 min gradient of 5% to 38% acetonitrile in 0.1% formic acid at a flow rate of 300 nL/min. The Orbitrap Velos was operated in positive ion mode with the nanospray voltage set at 1.5 kV and a source temperature of 275 °C. Internal calibration was performed with the background ion signal at m/z 445.120025 as the lock mass. The instrument was operated in parallel data-dependent acquisition mode using an FT mass analyzer for one survey MS scan for precursor ions followed by MS/MS scans on the top 7 highest intensity peaks with multiple charged ions above a threshold ion count of 7500 in both the LTQ mass analyzer and the high-energy collision dissociation (HCD)-based FT mass analyzer at 7500 resolution. Dynamic exclusion parameters were set at a repeat count of 1 with a 15 s repeat duration, an exclusion list size of 500, an exclusion duration of 30 s, and an exclusion mass width of ±10 ppm.

HCD parameters were set at the following values: isolation width of 2.0 m/z, normalized collision energy of 35%, activation Q at 0.25, and activation time of 0.1 ms. All data were acquired using Xcalibur operation software (version 2.1, ThermoFisher).

All MS and MS/MS raw spectra were processed and searched using Proteome Discoverer 1.3 (PD1.3; ThermoFisher) against databases downloaded from the NCBI database. The database search was performed with two-missed cleavage sites by trypsin allowed. The peptide tolerance was set to 10 ppm, and the MS/MS tolerance was set to 0.8 Da for collision-induced dissociation and 0.05 Da for HCD. A fixed carbamidomethyl modification of cysteine, variable modifications on methionine oxidation, and ubiquitin modification of lysine were set. The peptides with low confidence score (with an Xcorr score of <2 for doubly charged ions and <2.7 for triply charged ions) defined by PD1.3 were filtered out, and the remaining peptides were considered for the peptide identification with possible ubiquitination determinations. All MS/MS spectra for possibly identified ubiquitination peptides from initial database searching were manually inspected and validated using both PD1.3 and Xcalibur (version 2.1) software.

■ ASSOCIATED CONTENT

Supporting Information

The Supporting Information is available free of charge at https://pubs.acs.org/doi/10.1021/acssynbio.1c00357.

Expression and purification of uAbs; binding and ubiquitination activity of ERK-directed uAbs; expression and activity of ERK-targeting uAbs in living cells; silencing of pERK1/2 by EpE89 and pE59 uAbs; determination of poly-Ub chain architecture by ubiquitin profiling (PDF)

■ AUTHOR INFORMATION

Corresponding Author

Matthew P. DeLisa − *Biochemistry, Molecular and Cell Biology, Robert F. Smith School of Chemical and Biomolecular Engineering, and Nancy E. and Peter C. Meinig School of Biomedical Engineering, Cornell University, Ithaca, New York 14853, United States;* orcid.org/0000-0003-3226-1566; Phone: 607-254-8560; Email: md255@cornell.edu; Fax: 607-255-9166

Authors

Erin A. Stephens − *Biochemistry, Molecular and Cell Biology, Cornell University, Ithaca, New York 14853, United States*

Morgan B. Ludwicki − *Robert F. Smith School of Chemical and Biomolecular Engineering, Cornell University, Ithaca, New York 14853, United States*

Bunyarit Meksiriporn − *Nancy E. and Peter C. Meinig School of Biomedical Engineering, Cornell University, Ithaca, New York 14853, United States*

Mingji Li − *Robert F. Smith School of Chemical and Biomolecular Engineering, Cornell University, Ithaca, New York 14853, United States*

Tianzheng Ye − *Robert F. Smith School of Chemical and Biomolecular Engineering, Cornell University, Ithaca, New York 14853, United States*

Connor Monticello − *Nancy E. and Peter C. Meinig School of Biomedical Engineering, Cornell University, Ithaca, New York 14853, United States*

Katherine J. Forsythe − *College of Arts and Sciences, Cornell University, Ithaca, New York 14853, United States*

Lutz Kummer − *Department of Biochemistry, University of Zürich, 8057 Zürich, Switzerland*

Pengbo Zhou − *Department of Pathology and Laboratory Medicine, The Joan and Stanford I. Weill Medical College of Cornell University, New York, New York 10065, United States*

Andreas Plückthun − *Department of Biochemistry, University of Zürich, 8057 Zürich, Switzerland;* orcid.org/0000-0003-4191-5306

Complete contact information is available at: https://pubs.acs.org/10.1021/acssynbio.1c00357

Author Contributions

E.A.S. designed the research, performed all the research, analyzed all the data, and wrote the paper. M.B.L., B.M., M.L., and K.J.F. performed the research. T.Y., C.M., and P.Z. helped write and edit the paper. L.K. and A.P. aided in the data interpretation. M.P.D. directed the research, analyzed the data, and wrote the paper.

Notes

The authors declare the following competing financial interest(s): M.P.D. has a financial interest in UbiquiTx, Inc. M.P.D.'s interests are reviewed and managed by Cornell University in accordance with their conflict of interest policies. All other authors declare no competing interests.

https://doi.org/10.1021/acssynbio.1c00357
ACS Synth. Biol. 2021, 10, 2396−2408

All data generated or analyzed during this study are included in this Article (and its Supporting Information) or are available from the corresponding authors on reasonable request.

■ ACKNOWLEDGMENTS

We thank Dr. Cam Patterson, Dr. Mark Ostermeier, Dr. Amy Karlsson, and Dr. Melanie Cobb for plasmids used in this study. We also thank Dr. Peter Schweitzer and the BRC Genomics Facility at the Cornell Institute of Biotechnology for the sequencing experiments and Sheng Zhang and the Proteomics and Metabolomics Facility of the Biotechnology Resource Center of the Cornell Institute of Biotechnology for help with the mass spectrometry experiments. This work was supported by the National Science Foundation Grant CBET-1605242 (to M.P.D.), the National Institutes of Health Grant Numbers R21CA132223 and R01GM137314 (to M.P.D.), the Defense Threat Reduction Agency HDTRA1-20-10004 (to M.P.D.), the New York State Office of Science, Technology and Academic Research Distinguished Faculty Award (to M.P.D.), and the Cornell Technology Acceleration and Maturation (CTAM) Fund. The work was also supported by seed project funding (to M.P.D.) through the National Institutes of Health-funded Cornell Center on the Physics of Cancer Metabolism (supporting grant 1U54CA210184-01). The content is solely the responsibility of the authors and does not necessarily represent the official views of the National Cancer Institute or the National Institutes of Health. E.A.S. and M.B.L. were each supported by National Science Foundation Graduate Research Fellowships (grants DGE-1650441 and DGE-1144153, respectively) and Cornell Presidential Life Science Fellowships. M.B.L. was also supported by a Cornell Fleming Graduate Scholarship. B.M. was supported by a Royal Thai Government Fellowship.

■ REFERENCES

(1) Lai, A. C.; Crews, C. M. Induced protein degradation: an emerging drug discovery paradigm. *Nat. Rev. Drug Discovery* **2017**, *16* (2), 101−114.
(2) Chen, R. P.; Gaynor, A. S.; Chen, W. Synthetic biology approaches for targeted protein degradation. *Biotechnol. Adv.* **2019**, *37* (8), 107446.
(3) Lopez-Barbosa, N.; Ludwicki, M. B.; DeLisa, M. P. Proteome editing using engineered proteins that hijack cellular quality control machinery. *AIChE J.* **2020**, *66*, e16854.
(4) Crews, C. M. Targeting the undruggable proteome: the small molecules of my dreams. *Chem. Biol.* **2010**, *17* (6), 551−5.
(5) Arkin, M. R.; Wells, J. A. Small-molecule inhibitors of protein-protein interactions: progressing towards the dream. *Nat. Rev. Drug Discovery* **2004**, *3* (4), 301−17.
(6) Ciechanover, A. The ubiquitin-proteasome pathway: on protein death and cell life. *EMBO J.* **1998**, *17* (24), 7151−60.
(7) Pickart, C. M. Targeting of substrates to the 26S proteasome. *FASEB J.* **1997**, *11* (13), 1055−66.
(8) Neklesa, T. K.; Winkler, J. D.; Crews, C. M. Targeted protein degradation by PROTACs. *Pharmacol. Ther.* **2017**, *174*, 138−144.
(9) Deshaies, R. J. Protein degradation: Prime time for PROTACs. *Nat. Chem. Biol.* **2015**, *11* (9), 634−5.
(10) Schneekloth, J. S.; Fonseca, F. N.; Koldobskiy, M.; Mandal, A.; Deshaies, R.; Sakamoto, K.; Crews, C. M. Chemical genetic control of protein levels: selective in vivo targeted degradation. *J. Am. Chem. Soc.* **2004**, *126* (12), 3748−3754.
(11) Hines, J.; Gough, J. D.; Corson, T. W.; Crews, C. M. Posttranslational protein knockdown coupled to receptor tyrosine kinase activation with phosphoPROTACs. *Proc. Natl. Acad. Sci. U. S. A.* **2013**, *110* (22), 8942−7.
(12) Schneekloth, A. R.; Pucheault, M.; Tae, H. S.; Crews, C. M. Targeted intracellular protein degradation induced by a small molecule: En route to chemical proteomics. *Bioorg. Med. Chem. Lett.* **2008**, *18* (22), 5904−8.
(13) Bondeson, D. P.; Mares, A.; Smith, I. E.; Ko, E.; Campos, S.; Miah, A. H.; Mulholland, K. E.; Routly, N.; Buckley, D. L.; Gustafson, J. L.; Zinn, N.; Grandi, P.; Shimamura, S.; Bergamini, G.; Faelth-Savitski, M.; Bantscheff, M.; Cox, C.; Gordon, D. A.; Willard, R. R.; Flanagan, J. J.; Casillas, L. N.; Votta, B. J.; den Besten, W.; Famm, K.; Kruidenier, L.; Carter, P. S.; Harling, J. D.; Churcher, I.; Crews, C. M. Catalytic in vivo protein knockdown by small-molecule PROTACs. *Nat. Chem. Biol.* **2015**, *11* (8), 611−7.
(14) Sakamoto, K. M.; Kim, K. B.; Kumagai, A.; Mercurio, F.; Crews, C. M.; Deshaies, R. J. Protacs: chimeric molecules that target proteins to the Skp1-Cullin-F box complex for ubiquitination and degradation. *Proc. Natl. Acad. Sci. U. S. A.* **2001**, *98* (15), 8554−9.
(15) Mullard, A. First targeted protein degrader hits the clinic. *Nat. Rev. Drug Discovery* **2019**, *18*, 237−239.
(16) Zhou, P.; Bogacki, R.; McReynolds, L.; Howley, P. M. Harnessing the ubiquitination machinery to target the degradation of specific cellular proteins. *Mol. Cell* **2000**, *6* (3), 751−6.
(17) Zhang, J.; Zheng, N.; Zhou, P. Exploring the functional complexity of cellular proteins by protein knockout. *Proc. Natl. Acad. Sci. U. S. A.* **2003**, *100* (24), 14127−32.
(18) Kong, F.; Zhang, J.; Li, Y.; Hao, X.; Ren, X.; Li, H.; Zhou, P. Engineering a single ubiquitin ligase for the selective degradation of all activated ErbB receptor tyrosine kinases. *Oncogene* **2014**, *33* (8), 986−95.
(19) Ma, Y.; Gu, Y.; Zhang, Q.; Han, Y.; Yu, S.; Lu, Z.; Chen, J. Targeted degradation of KRAS by an engineered ubiquitin ligase suppresses pancreatic cancer cell growth in vitro and in vivo. *Mol. Cancer Ther.* **2013**, *12* (3), 286−94.
(20) Sufan, R. I.; Moriyama, E. H.; Mariampillai, A.; Roche, O.; Evans, A. J.; Alajez, N. M.; Vitkin, I. A.; Yang, V. X.; Liu, F. F.; Wilson, B. C.; Ohh, M. Oxygen-independent degradation of HIF-alpha via bioengineered VHL tumour suppressor complex. *EMBO Mol. Med.* **2009**, *1* (1), 66−78.
(21) Hatakeyama, S.; Watanabe, M.; Fujii, Y.; Nakayama, K. I. Targeted destruction of c-Myc by an engineered ubiquitin ligase suppresses cell transformation and tumor formation. *Cancer Res.* **2005**, *65* (17), 7874−9.
(22) Portnoff, A. D.; Stephens, E. A.; Varner, J. D.; DeLisa, M. P. Ubiquibodies, synthetic E3 ubiquitin ligases endowed with unnatural substrate specificity for targeted protein silencing. *J. Biol. Chem.* **2014**, *289* (11), 7844−55.
(23) Sheehan, J.; Marasco, W. A. Phage and yeast display. *Microbiol. Spectrum* **2015**, *3* (1), AID-0028-2014.
(24) Dreier, B.; Pluckthun, A. Rapid selection of high-affinity binders using ribosome display. *Methods Mol. Biol.* **2012**, *805*, 261−86.
(25) Colwill, K.; Renewable Protein Binder Working Group; Graslund, S. A roadmap to generate renewable protein binders to the human proteome. *Nat. Methods* **2011**, *8* (7), 551−558.
(26) Caussinus, E.; Kanca, O.; Affolter, M. Fluorescent fusion protein knockout mediated by anti-GFP nanobody. *Nat. Struct. Mol. Biol.* **2012**, *19* (1), 117−21.
(27) Ludwicki, M. B.; Li, J.; Stephens, E. A.; Roberts, R. W.; Koide, S.; Hammond, P. T.; DeLisa, M. P. Broad-spectrum proteome editing with an engineered bacterial ubiquitin ligase mimic. *ACS Cent. Sci.* **2019**, *5* (5), 852−866.
(28) Fulcher, L. J.; Hutchinson, L. D.; Macartney, T. J.; Turnbull, C.; Sapkota, G. P. Targeting endogenous proteins for degradation through the affinity-directed protein missile system. *Open Biol.* **2017**, *7* (5), 170066.
(29) Fulcher, L. J.; Macartney, T.; Bozatzi, P.; Hornberger, A.; Rojas-Fernandez, A.; Sapkota, G. P. An affinity-directed protein missile system for targeted proteolysis. *Open Biol.* **2016**, *6* (10), 160255.
(30) Shin, Y. J.; Park, S. K.; Jung, Y. J.; Kim, Y. N.; Kim, K. S.; Park, O. K.; Kwon, S. H.; Jeon, S. H.; Trinh le, A.; Fraser, S. E.; Kee, Y.;

https://doi.org/10.1021/acssynbio.1c00357
ACS Synth. Biol. 2021, 10, 2396−2408

Hwang, B. J. Nanobody-targeted E3-ubiquitin ligase complex degrades nuclear proteins. *Sci. Rep.* **2015**, *5*, 14269.
(31) Lim, S.; Khoo, R.; Peh, K. M.; Teo, J.; Chang, S. C.; Ng, S.; Beilhartz, G. L.; Melnyk, R. A.; Johannes, C. W.; Brown, C. J.; Lane, D. P.; Henry, B.; Partridge, A. W. bioPROTACs as versatile modulators of intracellular therapeutic targets including proliferating cell nuclear antigen (PCNA). *Proc. Natl. Acad. Sci. U. S. A.* **2020**, *117* (11), 5791−5800.
(32) Roth, S.; Macartney, T. J.; Konopacka, A.; Chan, K. H.; Zhou, H.; Queisser, M. A.; Sapkota, G. P. Targeting endogenous K-RAS for degradation through the affinity-directed protein missile system. *Cell Chem. Biol.* **2020**, *27* (9), 1151−1163.E6.
(33) Chatterjee, P.; Ponnapati, M.; Kramme, C.; Plesa, A. M.; Church, G. M.; Jacobson, J. M. Targeted intracellular degradation of SARS-CoV-2 via computationally optimized peptide fusions. *Commun. Biol.* **2020**, *3* (1), 715.
(34) Baltz, M. R.; Stephens, E. A.; DeLisa, M. P. Design and functional characterization of synthetic E3 ubiquitin ligases for targeted protein depletion. *Curr. Protoc Chem. Biol.* **2018**, *10* (1), 72−90.
(35) Busca, R.; Pouyssegur, J.; Lenormand, P. ERK1 and ERK2Map Kinases: Specific Roles or Functional Redundancy? *Front. Cell Dev. Biol.* **2016**, *4*, 53.
(36) Samatar, A. A.; Poulikakos, P. I. Targeting RAS-ERK signalling in cancer: promises and challenges. *Nat. Rev. Drug Discovery* **2014**, *13* (12), 928−42.
(37) Chambard, J. C.; Lefloch, R.; Pouyssegur, J.; Lenormand, P. ERK implication in cell cycle regulation. *Biochim. Biophys. Acta, Mol. Cell Res.* **2007**, *1773* (8), 1299−310.
(38) Yoon, S.; Seger, R. The extracellular signal-regulated kinase: multiple substrates regulate diverse cellular functions. *Growth Factors* **2006**, *24* (1), 21−44.
(39) Kummer, L.; Parizek, P.; Rube, P.; Millgramm, B.; Prinz, A.; Mittl, P. R.; Kaufholz, M.; Zimmermann, B.; Herberg, F. W.; Pluckthun, A. Structural and functional analysis of phosphorylation-specific binders of the kinase ERK from designed ankyrin repeat protein libraries. *Proc. Natl. Acad. Sci. U. S. A.* **2012**, *109* (34), E2248−57.
(40) Zhang, M.; Windheim, M.; Roe, S. M.; Peggie, M.; Cohen, P.; Prodromou, C.; Pearl, L. H. Chaperoned ubiquitylation–crystal structures of the CHIP U box E3 ubiquitin ligase and a CHIP-Ubc13-Uev1a complex. *Mol. Cell* **2005**, *20* (4), 525−38.
(41) Xu, Z.; Devlin, K. I.; Ford, M. G.; Nix, J. C.; Qin, J.; Misra, S. Structure and interactions of the helical and U-box domains of CHIP, the C terminus of HSP70 interacting protein. *Biochemistry* **2006**, *45* (15), 4749−59.
(42) Connell, P.; Ballinger, C. A.; Jiang, J.; Wu, Y.; Thompson, L. J.; Hohfeld, J.; Patterson, C. The co-chaperone CHIP regulates protein triage decisions mediated by heat-shock proteins. *Nat. Cell Biol.* **2001**, *3* (1), 93−6.
(43) Binz, H. K.; Amstutz, P.; Pluckthun, A. Engineering novel binding proteins from nonimmunoglobulin domains. *Nat. Biotechnol.* **2005**, *23* (10), 1257−68.
(44) Meksiriporn, B.; Ludwicki, M. B.; Stephens, E. A.; Jiang, A.; Lee, H. C.; Waraho-Zhmayev, D.; Kummer, L.; Brandl, F.; Pluckthun, A.; DeLisa, M. P. A survival selection strategy for engineering synthetic binding proteins that specifically recognize post-translationally phosphorylated proteins. *Nat. Commun.* **2019**, *10* (1), 1830.
(45) Qian, S. B.; Waldron, L.; Choudhary, N.; Klevit, R. E.; Chazin, W. J.; Patterson, C. Engineering a ubiquitin ligase reveals conformational flexibility required for ubiquitin transfer. *J. Biol. Chem.* **2009**, *284* (39), 26797−802.
(46) Khokhlatchev, A. V.; Canagarajah, B.; Wilsbacher, J.; Robinson, M.; Atkinson, M.; Goldsmith, E.; Cobb, M. H. Phosphorylation of the MAP kinase ERK2 promotes its homodimerization and nuclear translocation. *Cell* **1998**, *93* (4), 605−15.
(47) Pirkmajer, S.; Chibalin, A. V. Serum starvation: caveat emptor. *Am. J. Physiol Cell Physiol* **2011**, *301* (2), C272−9.
(48) Herrero, A.; Casar, B.; Colon-Bolea, P.; Agudo-Ibanez, L.; Crespo, P. Defined spatiotemporal features of RAS-ERK signals dictate cell fate in MCF-7 mammary epithelial cells. *Mol. Biol. Cell* **2016**, *27* (12), 1958−68.
(49) Giani, C.; Casalini, P.; Pupa, S. M.; De Vecchi, R.; Ardini, E.; Colnaghi, M. I.; Giordano, A.; Menard, S. Increased expression of c-erbB-2 in hormone-dependent breast cancer cells inhibits cell growth and induces differentiation. *Oncogene* **1998**, *17* (4), 425−32.
(50) Peng, J.; Schwartz, D.; Elias, J. E.; Thoreen, C. C.; Cheng, D.; Marsischky, G.; Roelofs, J.; Finley, D.; Gygi, S. P. A proteomics approach to understanding protein ubiquitination. *Nat. Biotechnol.* **2003**, *21* (8), 921−6.
(51) Dye, B. T.; Schulman, B. A. Structural mechanisms underlying posttranslational modification by ubiquitin-like proteins. *Annu. Rev. Biophys. Biomol. Struct.* **2007**, *36*, 131−50.
(52) Kundrat, L.; Regan, L. Identification of residues on Hsp70 and Hsp90 ubiquitinated by the cochaperone CHIP. *J. Mol. Biol.* **2010**, *395* (3), 587−94.
(53) Xu, P.; Duong, D. M.; Seyfried, N. T.; Cheng, D.; Xie, Y.; Robert, J.; Rush, J.; Hochstrasser, M.; Finley, D.; Peng, J. Quantitative proteomics reveals the function of unconventional ubiquitin chains in proteasomal degradation. *Cell* **2009**, *137* (1), 133−45.
(54) Saeki, Y.; Kudo, T.; Sone, T.; Kikuchi, Y.; Yokosawa, H.; Toh-e, A.; Tanaka, K. Lysine 63-linked polyubiquitin chain may serve as a targeting signal for the 26S proteasome. *EMBO J.* **2009**, *28* (4), 359−71.
(55) Osherovich, L. Degradation from within. *Science-Business Exchange* **2014**, *7*, 191.
(56) Ferrell, J. E., Jr. Tripping the switch fantastic: how a protein kinase cascade can convert graded inputs into switch-like outputs. *Trends Biochem. Sci.* **1996**, *21* (12), 460−466.
(57) Stankiewicz, M.; Nikolay, R.; Rybin, V.; Mayer, M. P. CHIP participates in protein triage decisions by preferentially ubiquitinating Hsp70-bound substrates. *FEBS J.* **2010**, *277* (16), 3353−67.
(58) Liu, F.; Yang, X.; Geng, M.; Huang, M. Targeting ERK, an Achilles' Heel of the MAPK pathway, in cancer therapy. *Acta Pharm. Sin. B* **2018**, *8* (4), 552−562.
(59) Chen, W.; Lee, J.; Cho, S. Y.; Fine, H. A. Proteasome-mediated destruction of the cyclin a/cyclin-dependent kinase 2 complex suppresses tumor cell growth in vitro and in vivo. *Cancer Res.* **2004**, *64* (11), 3949−57.
(60) Cohen, J. C.; Scott, D. K.; Miller, J.; Zhang, J.; Zhou, P.; Larson, J. E. Transient in utero knockout (TIUKO) of C-MYC affects late lung and intestinal development in the mouse. *BMC Dev. Biol.* **2004**, *4*, 4.
(61) Nicholes, N.; Date, A.; Beaujean, P.; Hauk, P.; Kanwar, M.; Ostermeier, M. Modular protein switches derived from antibody mimetic proteins. *Protein Eng., Des. Sel.* **2016**, *29* (2), 77−85.
(62) Mizrachi, D.; Chen, Y.; Liu, J.; Peng, H. M.; Ke, A.; Pollack, L.; Turner, R. J.; Auchus, R. J.; DeLisa, M. P. Making water-soluble integral membrane proteins in vivo using an amphipathic protein fusion strategy. *Nat. Commun.* **2015**, *6*, 6826.
(63) Ikonomova, S. P.; He, Z.; Karlsson, A. J. A simple and robust approach to immobilization of antibody fragments. *J. Immunol. Methods* **2016**, *435*, 7−16.
(64) Amstutz, P.; Koch, H.; Binz, H. K.; Deuber, S. A.; Pluckthun, A. Rapid selection of specific MAP kinase-binders from designed ankyrin repeat protein libraries. *Protein Eng., Des. Sel.* **2006**, *19* (5), 219−29.

https://doi.org/10.1021/acssynbio.1c00357
ACS Synth. Biol. 2021, 10, 2396−2408